Composites Part C: Open Access 8 (2022) 100284

Contents lists available at ScienceDirect

Composites Part C: Open Access

journal homepage: www.sciencedirect.com/journal/composites-part-c-open-access

Out-of-plane load-bearing and mechanical energy absorption properties of flexible density-graded TPU honeycombs

Ibnaj Anamika Anni [a], Kazi Zahir Uddin [a], Nicholas Pagliocca [a], Nand Singh [a,b], Oyindamola Rahman [a], George Youssef [c], Behrad Koohbor [a,b,*]

[a] Department of Mechanical Engineering, Rowan University, 201 Mullica Hill Rd., Glassboro, NJ 08028, United States
[b] Advanced Materials and Manufacturing Institute, Rowan University, Glassboro, NJ 08028, United States
[c] Experimental Mechanics Laboratory, Department of Mechanical Engineering, San Diego State University, 5500 Campanile Drive, San Diego, CA 92182, United States

ARTICLE INFO

Keywords:
Cellular structures
Additive manufacturing
Energy absorption
Thermoplastic polyurethane
Density gradation

ABSTRACT

Honeycomb structures are widely used in applications that require excellent strain energy mitigation at low structural weights. The load-bearing and energy absorption capacity of honeycomb structures strongly depend on their cell wall thickness to edge ratios. This work studies the mechanical response and strain energy absorption characteristics of hexagonal honeycomb structures with various cell wall thicknesses in response to out-of-plane loading conditions. Honeycomb structures with various nominal densities are first additively manufactured from flexible thermoplastic polyurethane (TPU). A comprehensive experimental study characterized the mechanical strength, energy absorption performance, and the strain recoverability of the structures. Density-graded structures are then fabricated by stacking multiple density layers of the honeycombs. Mechanical characterization of the density-graded structures points to their superior load-bearing response at large deformation conditions. From a strain energy absorption perspective, density graded structures are shown to outperform their uniform density counterparts at small deformation conditions. The results obtained in this work highlight the significance of density gradation as a practical means for the development of honeycomb structures with highly tailorable, application-specific mechanical properties.

1. Introduction

The ability to obtain tailorable mechanical and physical properties at significantly reduced structural weight has been the driving force behind cellular structures in various engineering applications, ranging from inexpensive packaging to the aerospace industry [1]. Furthermore, the tailorability of properties has been invigorated by advanced manufacturing. As a result, research trends on cellular structures have shifted towards fabricating structures with further improved properties and considerably lower densities due to advancements in additive manufacturing technologies and computational algorithms. As such, the design, development, and optimization of density-graded cellular structures has become a topic of great interest, attracting significant attention, and leading to some remarkable advancements, particularly in protective and impact mitigating structures [2].

Potential benefits of density gradation in cellular solids have been highlighted in several studies conducted on stochastic (*i.e.*, foams) and ordered (*e.g.*, honeycombs and other lattices) cellular structures [3–9]. Recent studies by Bates et al. [9] discussed the potentials of density gradation as a practical and viable approach for tailoring the damping properties and impact energy mitigation behaviors of honeycomb structures. It was shown in this work that flexible hexagonal honeycombs with various density gradations can be additively manufactured (*i.e.*, 3D printed) using the fused filament fabrication (FFF) process. When subjected to in-plane compressive loads, the density-graded structures outperformed their uniform density counterparts in terms of densification strain and specific stiffness in single-cycle and multi-cycle loading conditions. In line with the concepts discussed in Bates et al. [9], a recent study by the current authors highlighted the role of gradient functions on the variation of the mechanical load-bearing and energy absorption capacities of density-graded flexible honeycombs [6]. It was proven that regardless of the gradient function, density gradation is a practical strategy to increase the densification onset strain in honeycomb structures while maintaining or even reducing their overall density. Numerous theoretical, numerical, and experimental studies have been carried out to characterize the load-bearing capability and impact

* Corresponding author at: Department of Mechanical Engineering, Rowan University, 201 Mullica Hill Rd., Glassboro, NJ 08028, United States.
E-mail address: koohbor@rowan.edu (B. Koohbor).

https://doi.org/10.1016/j.jcomc.2022.100284
Received 3 April 2022; Received in revised form 5 May 2022; Accepted 24 May 2022
Available online 25 May 2022

energy absorption in density-graded cellular structures under high strain rate loading conditions [10–13]. These studies unanimously emphasize the promising potentials of density gradation in tailoring the mechanical response of cellular structures.

Additionally, density-graded honeycomb structures subjected to out-of-plane compressive loads have attracted some attention [14,15]. Considering the widespread use of honeycombs in sandwich structures, most research works in the literature studying the effect of density gradation on the out-of-plane response of honeycombs are applications-based and focus on the design and development of sandwich panels with graded foam and honeycomb cores [14,15]. However, from a fundamental mechanics perspective, the promising benefits of out-of-plane density gradation in honeycombs have only been realized and studied in a few recent publications [16–19]. For instance, tailoring of mechanical properties by the controlled variation of cell wall thickness along the honeycomb height has been discussed by Kumar et al. [19], where a continuous variation of cell-wall thickness from one face to another face of 3D printed honeycombs was associated with $a > 110\%$ increase in specific energy absorption. It was also shown that the gradient function, *i.e.*, the mathematical function that describes the length-wise variation of cell walls in a graded honeycomb, strongly influenced the overall load-bearing and energy absorption properties of the structures. Although recent studies demonstrated the design of graded honeycombs with highly controllable properties, major gaps exist in understanding the dichotomy between structural weight, geometric features, and mechanical performance in graded honeycombs subjected to out-of-plane loading. Furthermore, the state-of-the-art in this research area has only been limited to 3D printed structures made from rigid thermoplastic materials whose irrecoverable, permanent deformation limits their application to a single loading event [20].

The present study explores the roles of density gradation on the mechanical performance of additively manufactured honeycombs fabricated from flexible thermoplastic polyurethane (TPU). The underlying elastomeric nature of TPU highlights the potential reusability for multiple and repetitive loadings. The proposed reusability aspect can be particularly promising in packaging industries, wherein the application of honeycomb structures as lightweight energy absorbing components has been an active area of research for decades [21,22]. The research plan is designed based on a systematic approach that, first, investigates the mechanical and energy absorption behaviors of uniform density honeycomb structures with various cell wall thickness-to-edge ratios. The time-dependent recoverable shape and properties of the uniform density structures are investigated through the application of controlled cyclic compressive loads. Density-graded structures with discrete layers are then designed, fabricated, and characterized in terms of their load-bearing and energy absorption capacities. A comparison between the properties of the uniform density and graded structures is also conducted to determine the correlations between gradient schemes and mechanical performance.

2. Materials and methodology

2.1. Material selection

Thermoplastic polyurethane (TPU) was selected as the base polymer for sample fabrication. Mechanical properties of TPU have been widely studied in the literature [9], highlighting its unique combination of strength and flexibility, and its capabilities for use in extrusion-based additive manufacturing processes. The mechanical energy absorption capacity of 3D printed hexagonal honeycombs composed of TPU subjected to in-plane loading has also been investigated [2,9], pointing to its promising potentials as a strong material candidate for the purposes sought in the present work.

Tensile and compressive properties of neat TPU were characterized in-house for reference. To this end, ASTM D638 standard dog bone samples were 3D printed (Creality Ender 3 printer with a 0.4 mm nozzle diameter) using a fused filament fabrication instrument that raster deposited the molten TPU in directions parallel to the axis of the dog bone sample, and were tested in tension. For compression tests, cubic samples ($10 \times 10 \times 10$ mm) were prepared using the same printing method. While it is well understood the printing direction plays a major role in the mechanical performance of additively manufactured structures [23,24], the aforementioned printing direction was selected herein since it aligns with the direction the honeycomb structures were printed and tested. Tensile and compression tests were performed under nominal strain rates of 10^{-3} s^{-1} in a Shimadzu AGS-X unit equipped with a 10 kN load cell. **Fig. 1** shows the engineering stress-strain response of TPU under tensile and compressive loading conditions and exemplifies the sought-after elastomeric response for impact mitigation structures.

2.2. Cellular structure design and fabrication

This research designed, fabricated, and tested regular honeycomb structures with variable cell wall thicknesses and heights. All samples were designed in the SolidWorks® 2020 module and were manufactured using the same 3D printing methods described in **Section2.1**. Hexagonal honeycombs with an array of 7 hexagonal cells (**Fig. 2a** & **b**) were designed with cell wall thicknesses, t, ranging from 1 mm to 5 mm and a constant cell edge size, l, of 6 mm. Samples with heights, h, of 3.6 to 30 mm were designed and fabricated for different experimentation purposes. The sample height was fixed at 18 mm for all uniform density cellular structures.

Density graded samples were also produced with 2-stage, 3-stage, and 5-stage gradients (**Fig. 2c**). In the case of 2-stage graded structures, the 18 mm total height of sample was separated into two equi-height sections. The upper section was fabricated using a hexagonal honeycomb design with $t = 1$ mm, $l = 6$ mm, and $h = 9$ mm. The bottom segment was produced with the same cell edge and height sizes (*i.e.*, $l = 6$ mm and $h = 9$ mm) but with a thicker cell wall of $t = 5$ mm. Similarly, the 3-stage graded samples were fabricated with three equal height segments with $h = 6$ mm and $l = 6$ mm. The top, middle, and bottom segments of the 3-stage graded samples had cell wall thicknesses equal to 1 mm, 3 mm, and 5 mm, respectively. The 5-stage structures were produced according to the same concept, with five equal height segments ($h = 3.6$ mm), with cell wall thicknesses ranging from 1 mm to 5 mm from top to bottom. Load-bearing cross sectional areas associated with different cell wall thicknesses were determined and used for calculation of the nominal volume of the samples. **Table 1** shows the calculated cross sectional area and volume of the structures examined in this work. For mechanical testing of the graded structures, a thin layer of a hardened aluminum sheet was cut and placed between the layers of all graded structures to ensure the uniform stress distribution transferred from one density stage to another. The small elastic deformation of the Al sheets had negligible effect on the energy dissipation capacity of the graded structures.

2.3. Mechanical tests and characterization of energy absorption

All samples, including uniform and graded density structures, were subjected to out-of-plane compressive loads applied in the -z direction (**Fig. 2**). Mechanical testing of the honeycomb structures was conducted in a Shimadzu AGS-X test frame with a 100 kN load cell capacity and under a displacement-controlled mode. All tests were performed at a constant cross-head speed of 5 mm.min^{-1}. In all cases, samples were deformed to a maximum of *ca.* 80% of their original height, equivalent to an engineering strain of 0.8. Force-stroke data was collected at a rate of 1 Hz and used for load-bearing and energy absorption performance characterizations.

Specific energy absorption (*i.e.*, energy absorption normalized by volume) of the structures was determined using the following equation,

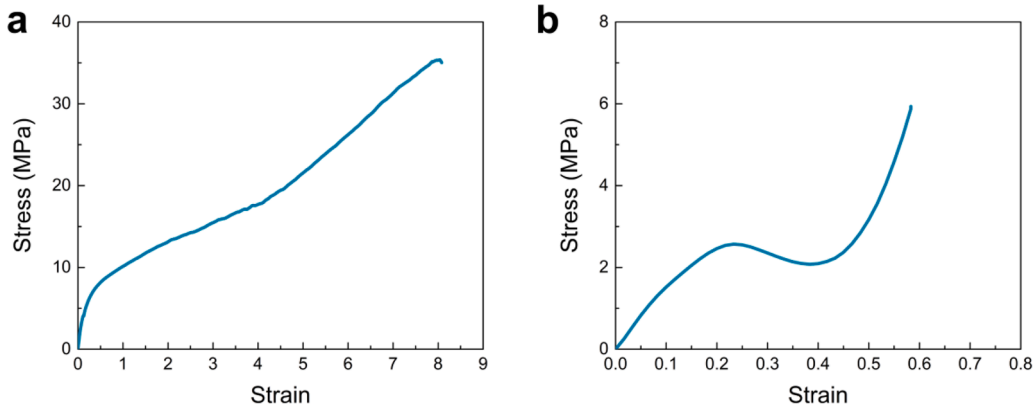

Fig. 1. Stress-strain response of thermoplastic polyurethane (TPU) base polymer in (a) tension and (b) compression.

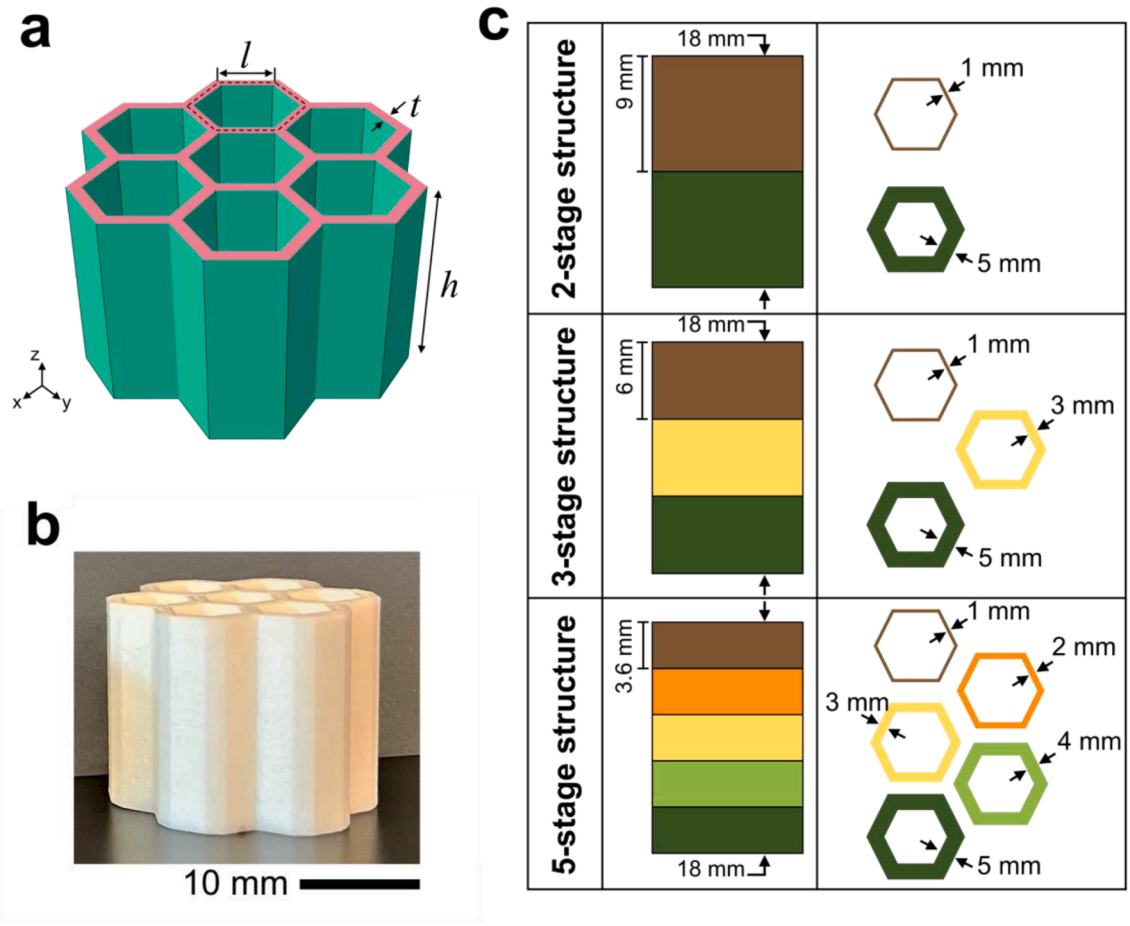

Fig. 2. (a) Geometric features of the honeycomb structures examined in this work. Uniform density structures were designed with a constant, *t*, along the height. An as-printed uniform density structure is shown in (b). For density graded structures, cell wall thickness, *t*, was varied in a step-wise manner as shown schematically in (c). cell edge size, *l*, was kept constant (=6 mm) for all structures, including uniform density and graded structures.

$$W = \frac{\int_0^{\delta} F.d\delta}{V}. \quad (1)$$

Where, W denotes the specific energy absorbed by the structure, F is the compressive force, and δ is the deformation (stroke) corresponding to the compressive force. V represents the nominal volume of the structures, listed in Table 1. The energy absorption efficiency of the structures, E, was determined using Eq. (2) as the ratio between the specific energy absorbed (W) and the compressive force at which the energy absorption is calculated [25].

$$E = \frac{W}{F.\delta} \quad (2)$$

3. Results and discussion

3.1. Deformation and energy absorption of uniform density structures

Fig. 3 shows the force-stroke curves obtained from compression testing of the uniform density structures. The overall shape of the curves

Table 1
Geometric features including the load-bearing cross-sectional area and the nominal density of the uniform density and graded structures.

	Structure	t (mm)	l (mm)	Total height, h (mm)	Load-bearing cross-sectional area (mm^2)	Volume (mm^3)
Uniform density	1 mm	1	6	18	190.6	3431.2
	2 mm	2			401.1	7218.9
	3 mm	3			633.5	11,403.4
	4 mm	4			885.4	15,936.3
	5 mm	5			1159.5	20,870.3
Density graded	2-stage	Variable along sample height			Variable along sample height	11,403.4
	3-stage					
	5-stage					

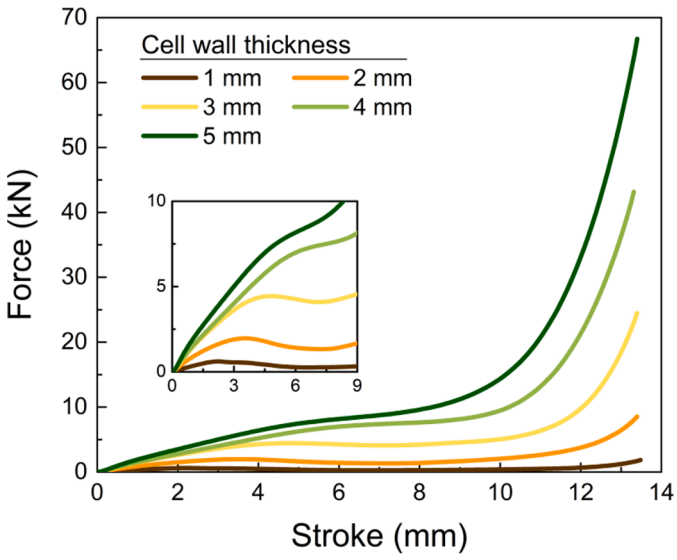

Fig. 3. Experimental force-stroke curves obtained for uniform density structures with various cell wall thicknesses. All structures in this plot have a height of 18 mm.

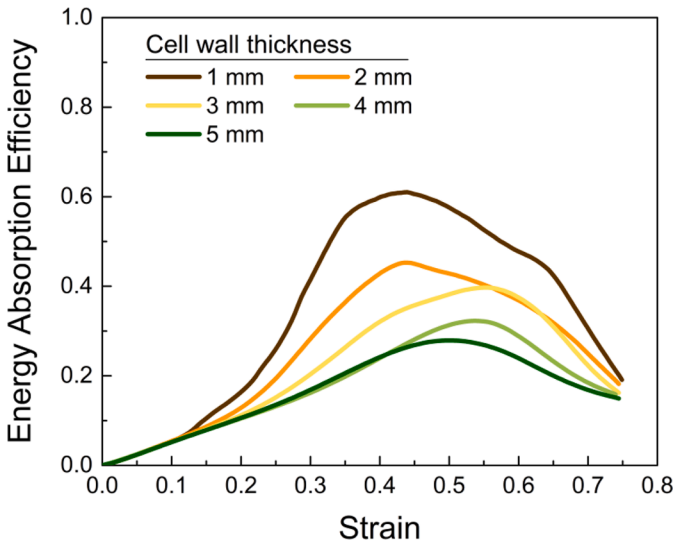

Fig. 4. Energy absorption efficiency *versus* strain curves for uniform density structures with different cell wall thicknesses.

is exemplified by an initial linear deformation regime whose slope indicates the nominal stiffness of the structure. The linear deformation regime develops into a plateau. The onset of the plateau region marks the beginning of cell wall instability, which in the case of the examined samples, is dominated by an elastic buckling mechanism [1]. Both stiffness and plateau forces depend on the wall thickness-to-cell edge ratio (t/l) of the structure. However, the plateau force (and its associated stress) has a stronger dependence on the t/l ratio, as also was proven by the theoretical solutions of Ashby and Gibson [1]. A local force peak and a slight decrease in force accompanies the transition from linear elastic to plateau regions, which is only seen for the three thinner cell walls. This observation is consistent with previous observations and is associated with the onset of buckling instability in thinner cell walls.

The end of the plateau region is marked by the onset of densification, shown in **Fig. 3** by a rapid force increase. The densification onset has been used as one of the practical metrics for determining of strain energy absorption capacity in honeycomb structures [6]. This parameter can be identified for a structure where the energy absorption efficiency is maximized [6]. Accordingly, the energy absorption efficiency parameter was determined for the uniform density structures using **Eq. (2)**. **Fig. 4** shows the variation of this parameter plotted with respect to strain. In this figure, strain is calculated by normalizing the compressive stroke with the initial 18 mm height of the structures.

All efficiency curves illustrated in **Fig. 4** show a single peak at a strain window of 0.45–0.55, implying a negligible effect of cell wall thickness on the densification strain. However, the efficiency values strongly depend on the cell wall thickness, with the thinner wall sections showing higher energy absorbing efficiencies. Because the thinner structures possess lighter weights and lower load bearing capacities, it would be reasonable to assume that a carefully designed graded structure made from a finite number of layers with variable wall thickness may lead to an optimal load-bearing and energy absorption performance that can be tailored for specific applications. This idea has been further explored in the forthcoming sections.

3.2. Viscoelastic behavior and strain recovery

A fundamental justification of this work is to leverage the hyperviscoelastic behavior of the base TPU material in creating structures that could sustain multiple strokes with full (or at least partial) recovery between the deformation events. Here, the hyperelastic behavior gives rise to increased stroke before densification, *i.e.*, improving the energy absorption efficacy of the structure. On the other hand, the viscoelastic response of TPU is desirable for repetitive loading, based on the recovery attributes and testing temperatures [26]. While a detailed analysis of the deformation recovery of the present samples requires an in-depth viscoelasticity analysis, the phenomenological strain recovery is studied by submitting the samples to compressive loads, and then allowing them to recover over time. Uniform density structures described in **Section 2.2** were utilized for this purpose. After loading to *ca.* 80% compression, the samples were unloaded and allowed to experience natural strain recovery in ambient conditions. The heights of the structures were measured periodically and after resting periods, starting immediately after unloading, *i.e.*, time = 0. Sample heights were also measured after 1.5 h, 3.5 h, 12 h, 24 h, and 72 h resting periods. **Fig. 5** shows the variation of recovered sample heights after the resting time periods, plotted in logarithmic time scales. Samples with thinner wall thicknesses are shown to have recovered quickly after unloading. Recovery is almost immediate for thinner cell wall structures (*e.g.*, $t = 1$, 2

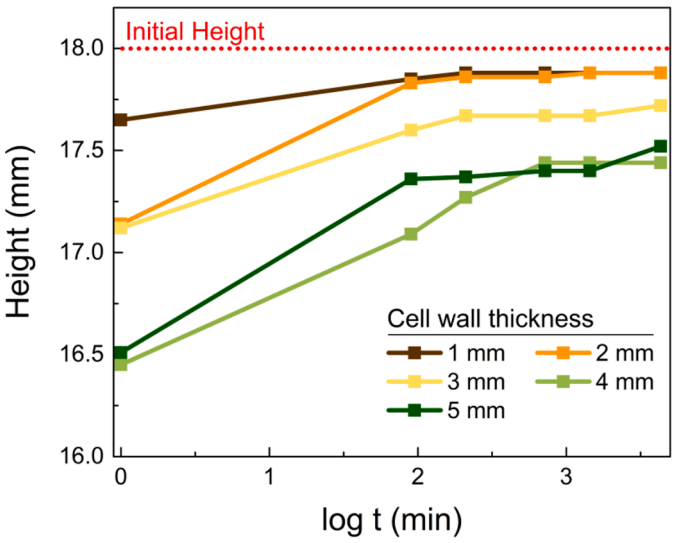

Fig. 5. Time-dependent recovery of uniform density structures after 80% compression. Samples tested all had an initial height of 18 mm. $t = 0$ indicates the sample height immediately after unloading.

mm) and remains nearly independent of the time after the first 1.5 h resting period. For example, samples with $t = 1$ mm reported a recovered height after loading representing ~97% of the initial sample height. Lower degrees of height recovery are measured for structures with thicker cell walls over the same periods. Although not completely recovered over the 72 h time resting time periods examined, all thick-walled samples show >91% immediately after unloading and >96% recovery after 72 h of resting. The irrecoverable height is likely due to the highly localized strains that lead to permanent set and internal damage formation in the structures. The formation of localized high strain regions may be associated with material viscous flow and printing defects [9,27], excessive local deformation due to fold and kink band formation (discussed in the forthcoming sections), or both. While the nature and characteristics of such irrecoverable strains and possible damage mechanisms are beyond the scope of this work, the significant height recovery of the structures is indicative of their capacity for use in multiple deformation events.

3.3. Effect of structure height on deformation response

Before embarking on further details about the design and development of graded structures, it is important to highlight the role of sample height as another independent variable. The role of this parameter on the load-bearing response of hexagonal honeycombs under out-of-plane compression has been studied by Gibson and Ashby [1]. The significance of sample height is primarily in controlling the degree of freedom of the vertical edges in response to the buckling load. Specifically, for cases with relatively large heights (*i.e.*, $h > 3l$), the vertical edges can be assumed to be simply supported, thus, free to rotate. Depending on the sample height to cell edge ratio, the vertical edges can be assumed as partially or fully clamped in shorter structures. In such cases, the critical force (and its associated stress) required to initiate the buckling mechanism increase [1]. To highlight the role of sample height, we show in **Fig. 6** the variation of force and energy absorption efficiency as functions of strain for various sample heights. Note that the results presented in this figure are obtained for constant cell wall thickness, t, and cell edge size, l, of 3 mm and 6 mm, respectively. **Fig. 6a** shows the force *versus* strain curves obtained for structures with various cell edge heights. Since the latter ranged between 12 mm and 36 mm, the stroke (displacement) values are normalized by the sample height to facilitate direct comparison between different cases in **Fig. 6a**. In line with the theory presented in [1], the load-bearing response remains independent of the sample height for the three taller structures, *i.e.*, those with $h = 24$, 30, 36 mm. On the other hand, the variation of the buckling mechanisms is reflected on the force-displacement data by discernible alterations in the overall shape and the quantitative values of the force-strain data. In particular, for the three taller structures, an apparent softening behavior is observed at strains equal to 0.3. The drop in the load-bearing capacity observed in these structures is characteristic of kinking due to compressive instability of the structures [28]. The height-dependent variations in the mechanical properties are also evident in the efficiency-strain curves shown in **Fig. 6b**, suggesting a drastic decrease in the energy absorption efficiency at reduced sample heights. Nevertheless, the strain associated with the maximum efficiency (*i.e.*, the densification onset strain) remains nearly constant and independent of the sample height, at least for the heights examined in this work.

The height-dependent mechanical behavior was further analyzed for other cell wall thicknesses and through *in-situ* imaging. For brevity and consistency, height-dependent mechanical data for other sample thicknesses are not elaborated here. However, the *in-situ* imaging results for the 3 mm cell wall thickness structures with various heights are presented in **Fig. 7** to accompany the discussions relevant to the underlying deformation mechanisms. The out-of-plane compression of the two shorter structures, *i.e.*, those with $h = 12$ and 18 mm, shows a more uniform buckling response, illustrated by the development of a significant barreling behavior at strains >0.2. In the case of the three taller samples, *i.e.*, those with $h = 24$, 30, and 36 mm, similar buckling responses are observed at strains <0.2. This deformation range

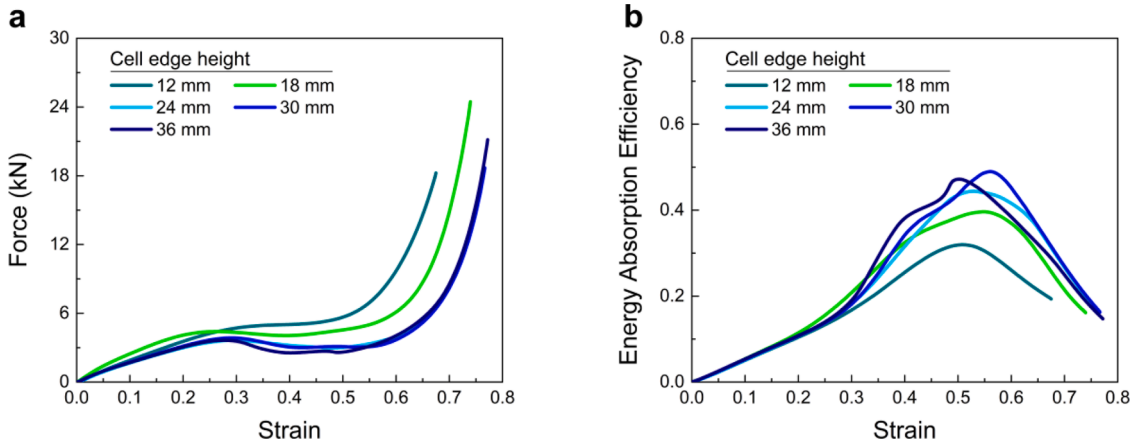

Fig. 6. (a) Force and (b) energy absorption efficiency *versus* strain for uniform density structures with different cell edge heights. Cell wall thickness and edge size in all cases are 3 and 6 mm, respectively.

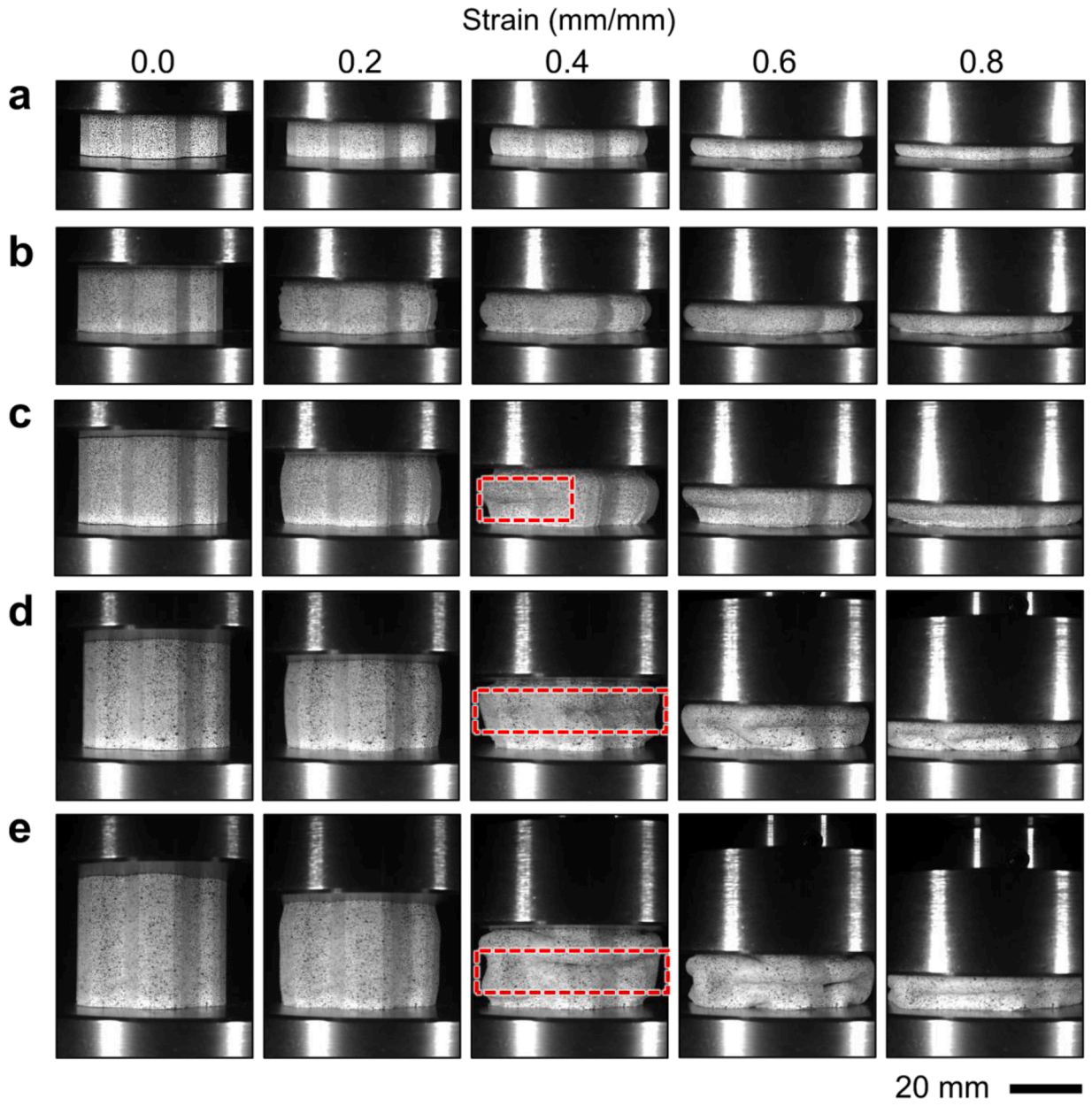

Fig. 7. Images showing the deformation evolution in structures with an initial height, *h*, of (a) 12 mm, (b) 18 mm, (c) 24 mm, (d) 30 mm, and (e) 36 mm. Cell wall thickness. *t*, in all cases is 3 mm. Evidence for compressive instability in the form of kink bands is marked with dashed rectangles. The dotted pattern on the surface of the structures was applied intentionally to increase contrast and facilitate higher quality imaging.

corresponds with the increasing force values shown earlier in Fig. 6**a**. However, at strains beyond 0.2, the formation of kink bands (marked by dashed rectangles in Fig. 7**c–e**) becomes evident, altering the overall deformation response from a uniform buckling mode to non-uniform buckling with inelastic folds and kink bands formed near the mid-height of the structures. Such folds and kink bands are consistent with previous observations on honeycombs fabricated from elasto-plastic base materials and are attributed to an increased energy absorption performance of the structure in response to out-of-plane compressive loads [29]. The improved energy absorption efficiency for the taller samples was shown and discussed in Fig. 6**b**. Note that the strain recovery in the presence of kink bands was not assessed for all sample heights. However, based on the results discussed in Section 3.2, it is reasonable to assume that if given enough time, the taller structures will recover even after the formation of kink bands. Nonetheless, the inelastic nature of the kink bands developed in taller samples may penalize their use in repetitive loading events.

3.4. Deformation and energy absorption of density-graded structures

Fig. 8 shows the force-stroke results for density-graded structures. To facilitate direct comparison, the force-stroke curves for uniform density structures (*i.e.*, from Fig. 3) are also included in the plot. The force-stroke response of the density graded structures shows a nonlinear trend at small deformations due to the distinct yielding of each of the respective density layers present in the structure. The observed stepwise yielding is consistent with the literature on both graded foams and functionally graded lattices [2,5,6,9,30,31]. The deformation mechanism is described by sequential linear deformations between layers. This is also rationalized by considering the stacked graded structures as springs, with different stiffness based on the structural attributes, arranged in series. Upon increase of the compressive load beyond the

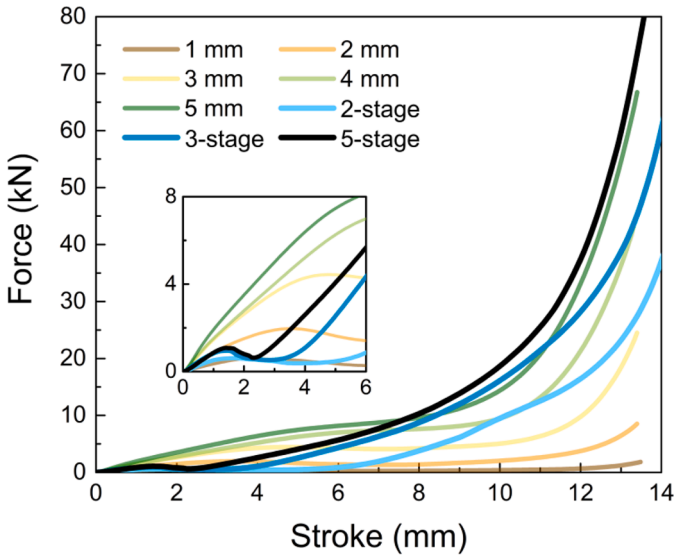

Fig. 8. Force-stroke curves obtained for density graded structures. Curves obtained for uniform density structures are also included for direct comparison.

apparent yield strength of the lowest density layer, the layer reaches a plateau. The deformation continues by successive yielding of the higher density layers until all of the layers in the structure reach their corresponding plateaus. Such stepwise deformation patterns can be readily observed in the response of the 2-stage graded structure in Fig. 8, where visible changes in concavity of the force-stroke response exist. As more density layers (herein referred to as 'stages') are added, the distinct stepwise yielding behavior vanishes and is substituted by a near-continuous yielding behavior that corresponds to the sequential yielding of multiple layers in the structure. For all of the examined graded structures, an improvement in load-bearing response at larger deformation and an enhancement in the apparent stiffness compared with the uniform density structures were observed. The force-stroke results support the advantages of spatial gradation for tuning the load-bearing response of honeycombs subjected to out-of-plane compressive loads.

A comparison between the specific energy absorption and energy absorption efficiency responses of the graded structures and their equivalent uniform density structure ($t = 3$ mm) is provided in Fig. 9. Examination of the specific energy absorption in Fig. 9**a** reveals that (1) although inferior to the uniform density structure at strains <0.5, the 3-stage and 5-stage graded structures outperform their uniform density counterparts in terms of energy absorption capacity at large strains. (2) A higher number of density stages result in an improved specific energy absorption. This behavior can be readily observed by comparing the specific energy absorption responses of 3- and 5-stage structures with the 2-stage graded structure. This trend would continue and converge to a specific value as the number of layers approaches infinity, *i.e.,* continuous gradation [9,19].

Fig. 9**b** & **c** show the variation of energy absorption efficiency plotted with respect to strain and force, respectively, for graded structures and their uniform density counterpart. Considering the peak

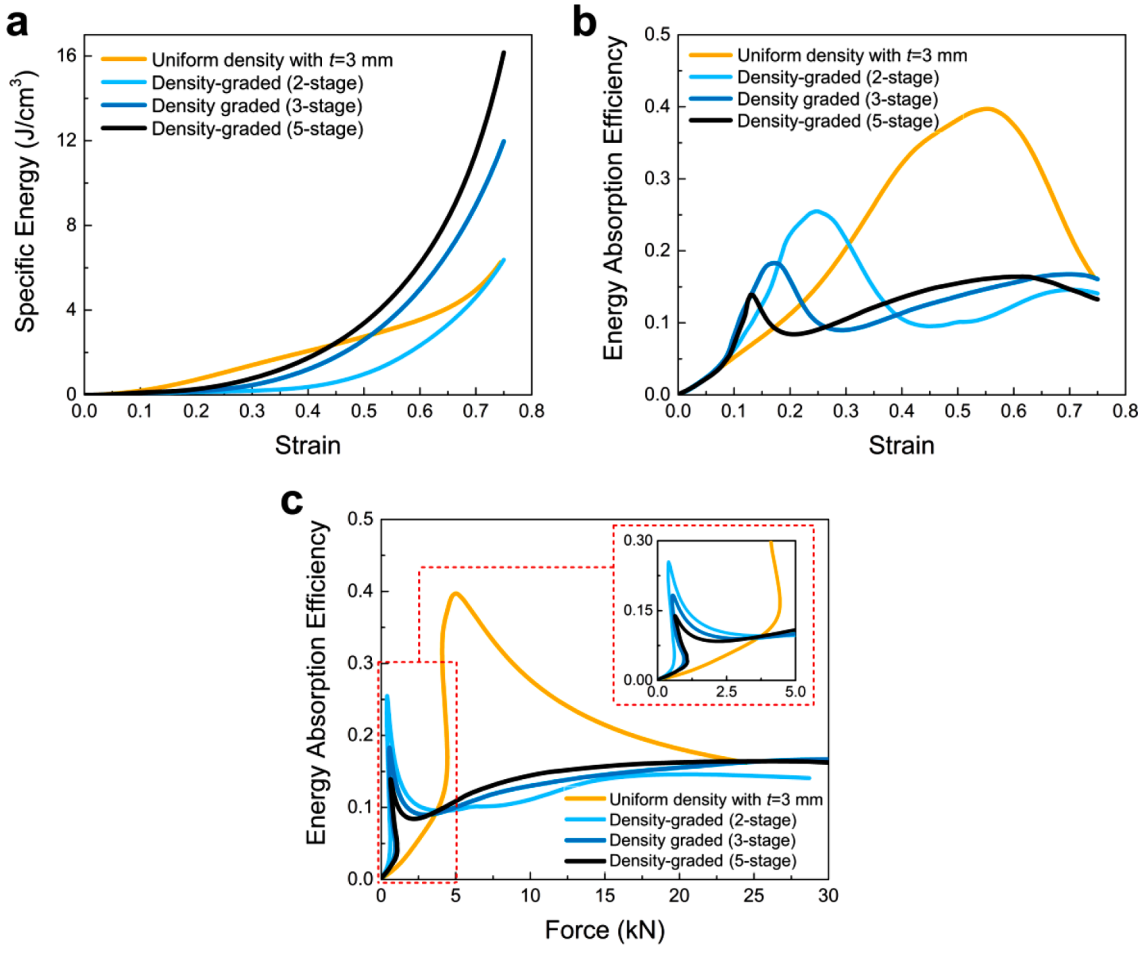

Fig. 9. (a) Specific energy absorption, *W*, and (b) energy absorption efficiency, *E*, of the graded structures plotted with respect to strain. (c) Energy absorption efficiency *versus* the applied force for graded structures. For comparison, curves obtained for the uniform density structure with $t = 3$ mm have been plotted, as well.

efficiency values in Fig. 9**b**, it is evident that the maximum efficiency for the graded structures is lower in value and is reached at smaller strain compared with the uniform density structure. Nevertheless, among all the graded structures examined in this work, the 2-stage structure outperforms the other two examined graded structures. It is also noted that increasing the number of density layers in the graded structures shifts the efficiency peaks to lower stain values. Likewise, all graded structures outperform the energy absorption efficiency of the uniform single-density structure at lower compressive forces, as clearly shown in Fig. 9**c**. The latter two observations suggest that density gradation has the potential to increase the energy absorption efficiency of honeycombs in small deformation conditions, an idea that can be appealing for their use in real-world applications such as packaging industries.

To further interpret the results discussed in this section, it is worth noting that the promising potentials of density gradation in honeycomb structures must be realized in terms of the applications sought for the structure. For applications wherein the applied loads and deformations tend to be higher, graded structures can perform better in terms of load-bearing and the amount of energy absorbed before failure. In particular, a higher number of density layers leads to further improvements in the load-bearing capacity of the structure, resulting in lower energy efficiency values (see Eq. (2) and Fig. 9**b**). Moreover, the concurrent improvements in energy absorption and mechanical strength occur at the expense of densification strain. On the other hand, for small deformation conditions, a uniform density structure with an equivalent density may be a better choice, as it offers higher strength (see Fig. 8) and higher energy absorption performance. Such application-specific strength-energy absorption dichotomies have been highlighted in previous studies for other types of cellular solids, including origami structures [32] and a variety of sheet-based and planar lattices [27,33]. Nevertheless, as suggested by the findings of the present study, density gradation can be a promising practical strategy for the design and development of lightweight structures with highly tunable mechanical and energy mitigation properties. A promising addition to the above characteristics is the structures' recovery of their original shape and properties, an ability that further improves the functionality of this novel class of structures for several industries. Last but not least, it should be emphasized that although discontinuous gradation is easier to achieve in practice, the geometric discontinuities at the layers' interfaces increase the propensity of stress concentration. Extending the concepts discussed herein into the design and development of continuous gradients is a topic of great interest for future studies.

4. Conclusions

The load-bearing and energy absorption requirements in impact mitigation applications align with the performance of density-grade honeycomb structures. This works demonstrated the tailorability of the mechanical performance of additively manufactured flexible honeycomb structures by adjusting the geometrical attributes of the unit cell. Two sets of structures were produced using fused filament fabrication method and flexible thermoplastic polyurethane, based on the hyper-viscoelastic of the latter in support of large and repetitive loading scenarios. The first set of honeycomb structures were single-density with different wall-thickness to height ratio. The second set consisted of density graded structures by altering the geometrical attributes of the structure. The results substantiate the significance of density gradation in controlling the load-bearing and energy absorption behavior of additively manufactured honeycombs. The density graded structures outperformed in load-bearing at large deformation and energy absorption at the other end of the deformation spectrum. While the outcomes are promising for impact mitigating applications, future studies will emphasize the source of deformation and damage mechanism as well as the possible reinforcement of material during printing.

Data availability

Data will be available upon request.

Declaration of Competing Interest

The authors declare that they have no known competing financial interests or personal relationships that could have appeared to influence the work reported in this paper.

Acknowledgments

The authors gratefully acknowledge the financial support from the Advanced Materials and Manufacturing Institute (AMMI) at Rowan University. The research leading to this publication was partially supported by the National Science Foundation under Grant No. 2035660 (B. K.) and Grant No. 2035663 (G.Y.).

References

[1] L.J. Gibson, M.F. Ashby, Cellular Solids: Structure and Properties, 2nd ed., Cambridge University Press, 1997.
[2] O. Rahman, K.Z. Uddin, J. Muthulingam, G. Youssef, C. Shen, B. Koohbor, Density-graded cellular solids: mechanics, fabrication and applications, Adv. Eng. Mater. 24 (2022), 2100646.
[3] N. Gupta, A functionally graded synthetic foam material for high energy absorption under compression, Mater. Lett. 61 (2007) 979–982.
[4] B. Koohbor, A. Kidane, Design optimization of continuously and discretely graded foam materials for efficient energy absorption, Mater. Des. 102 (2016) 151–161.
[5] B. Koohbor, S. Ravindran, A. Kidane, In situ deformation characterization of density-graded foams in quasi-static and impact loading conditions, Int. J. Impact Eng. 150 (2021), 103820.
[6] O. Rahman, B. Koohbor, Optimization of energy absorption performance of polymer honeycombs by density gradation, Compos. C 3 (2020), 100052.
[7] S.A. Galehdari, M. Kadkhodayan, S. Hadidi-Moud, Analytical, experimental and numerical study of a graded honeycomb structure under in-plane impact load with low velocity, Int. J. Crashworthiness 20 (2015) 387–400.
[8] D. Mousanezhad, R. Ghosh, A. Ajdari, A.M.S. Hamouda, H. Nayeb-Hashemi, A. Vaziri, Impact resistance and energy absorption of regular and functionally graded hexagonal honeycombs with cell wall material strain hardening, Int. J. Mech. Sci. 89 (2014) 413–422.
[9] S.R.G. Bates, I.R. Farrow, R.S. Trask, Compressive behaviour of 3D printed thermoplastic polyurethane honeycombs with graded densities, Mater. Des. 162 (2019) 130–142.
[10] J. Zhang, G. Lu, D. Ruan, X. Huang, Experimental observations of the double shock deformation mode in density graded honeycombs, Int. J. Impact Eng. 134 (2019), 103386.
[11] C.J. Shen, G. Lu, T.X. Yu, Dynamic behavior of graded honeycombs – a finite element study, Compos. Struct. 98 (2013) 282–293.
[12] Y. Duan, X. Zhao, Z. Liu, N. Hou, H. Liu, B. Du, B. Hou, Y. Li, Dynamic response of additively manufactured graded foams, Compos. B 183 (2020), 107630.
[13] D. Qi, Q. Lu, C.W. He, Y. Li, W. Wu, D. Xiao, Impact energy absorption of functionally graded chiral honeycomb structures, Extreme Mech. Lett. 32 (2019), 100568.
[14] L. Jing, X. Su, D. Chen, F. Yang, Z. Zhao, Experimental and numerical study of sandwich beams with layered-gradient foam cores under low-velocity impact, Thin-Walled Struct. 135 (2019) 227–244.
[15] Y. Tao, S. Duan, W. Wen, Y. Pei, D. Fang, Enhanced out-of-plane crushing strength and energy absorption of in-plane graded honeycombs, Compos. B 118 (2017) 33–40.
[16] G. Zhu, S. Li, G. Sun, G. Li, Q. Li, On design of graded honeycomb filler and tubal wall thickness for multiple load cases, Thin-Walled Struct. 109 (2016) 377–389.
[17] S. Duan, Y. Tao, H. Lei, W. Wen, J. Liang, D. Fang, Enhanced out-of-plane compressive strength and energy absorption of 3D printed square and hexagonal honeycombs with variable-thickness cell edges, Extreme Mech. Lett. 18 (2018) 9–18.
[18] Y. Wu, L. Sun, P. Yang, J. Fang, W. Li, Energy absorption of additively manufactured functionally bi-graded thickness honeycombs subjected to axial loads, Thin-Walled Struct. 164 (2021), 107810.
[19] S. Kumar, J. Ubaid, R. Abishera, A. Schiffer, V.S. Deshpande, Tunable energy absorption characteristics of architected honeycombs enabled via additive manufacturing, ACS Appl. Mater. Interfaces 11 (2019) 42549–42560.
[20] M.R. Khosravani, A. Zolfagharian, M. Jennings, T. Reinicke, Structural performance of 3D-printed composites under various loads and environmental conditions, Polym. Test 91 (2020), 106770.
[21] K. Li, J. Wang, L. Lu, Q. Qin, J. Chen, C. Shen, M. Jiang, Mechanical properties and energy absorption capability of a new multi-cell lattice honeycomb paperboard under out-plane compression: experimental and theoretical studies, Packag. Technol. Sci. 35 (3) (2022) 273–290.

[22] Z.W. Wang, L.J. Wang, C.Y. Xu, Y. Zhang, Influence of low-intensity repeated impacts on energy absorption and vibration transmissibility of honeycomb paperboard, Packaging Technol. Sci. 29 (2016) 585–600.
[23] N.U. Huynh, J. Smilo, A. Blourchian, A.V. Karapetian, G. Youssef, Property-map of epoxy-treated and as-printed polymeric additively manufactured materials, Int. J. Mech. Sci. 181 (2020), 105767.
[24] G. Youssef, J. Smilo, A. Blourchian, N.U. Huynh, A.V. Karapetian, Multifunctional fused deposition modeled acrylonitrile butadiene styrene-based structures with embedded conductive channels, J. Eng. Mater. Technol. 143 (2021), 011001.
[25] K.Z. Uddin, G. Youssef, M. Trkov, H. Seyyedhosseinzadeh, B. Koohbor, Gradient optimization of multi-layered density-graded foam laminates for footwear material design, J. Biomech. 109 (2020), 109950.
[26] G. Youssef, Applied Mechanics of Polymers: Properties, Processing, and Behavior, Elsevier, 2021.
[27] N. Pagliocca, K.Z. Uddin, I.A. Anni, C. Shen, G. Youssef, B. Koohbor, Flexible planar metamaterials with tunable Poisson's ratios, Mater. Des. 215 (2022), 110446.
[28] M. Vural, G. Ravichandran, Microstructural aspects and modeling of failure in naturally occurring porous composites, Mech. Mater. 35 (2003) 523–536.
[29] M.K. Khan, T. Baig, S. Mirza, Experimental investigation of in-plane and out-of-plane crushing of aluminum honeycomb, Mater. Sci. Eng. A 539 (2012) 135–142.
[30] X. Yu, Q. Qin, J. Zhang, S. He, C. Xiang, M. Wang, T. Wang, Crushing and energy absorption of density-graded foam-filled square columns: experimental and theoretical investigations, Compos. Struct. 201 (2018) 423–433.
[31] S. He, Y. Lv, S. Chen, G. Dai, J. Liu, M. Huo, Gradient regulation and compressive properties of density-graded aluminum foam, Mater. Sci. Eng. A 772 (2020), 138658.
[32] S. Townsend, R. Adams, M. Robinson, B. Hanna, P. Theobald, 3D printed origami honeycombs with tailored out-of-plane energy absorption behavior, Mater. Des. 195 (2020), 108930.
[33] O. Al-Ketan, D.-.W. Lee, R. Rowshan, R.K Abu Al-Rub, Functionally graded and multi-morphology sheet TPMS lattices: design, manufacturing, and mechanical properties, J. Mech. Behav. Biomed. Mater. 102 (2020), 103520.